

ADAPTIVE SAMPLING STRATEGIES FOR RISK-AVERSE STOCHASTIC OPTIMIZATION WITH CONSTRAINTS*

FLORIAN BEISER[†], BRENDAN KEITH[‡], SIMON URBAINCZYK[§], AND BARBARA WOHLMUTH[¶]

Abstract. We introduce adaptive sampling methods for risk-neutral and risk-averse stochastic programs with deterministic constraints. In particular, we propose a variant of the stochastic projected gradient method where the sample size used to approximate the reduced gradient is determined a posteriori and updated adaptively. We also propose an SQP-type method based on similar adaptive sampling principles. Both methods lead to a significant reduction in cost. Numerical experiments from finance and engineering illustrate the performance and efficacy of the presented algorithms. The methods here are applicable to a broad class of expectation-based risk measures, however, we focus mainly on expected risk and conditional value-at-risk minimization problems.

Key words. stochastic optimization, sample size selection, constrained optimization, portfolio optimization, shape optimization

AMS subject classifications. 90C15, 90C55, 62P30, 35Q93, 49Q10

1. Introduction. In this article, we consider the following general class of stochastic programs:

$$(1.1) \quad \min_{x \in C} \left\{ F(x) = \mathcal{R}[f(x; \xi)] \right\}.$$

Here, $f : \mathbb{R}^n \rightarrow \mathbb{R}$ is a smooth function, ξ is a random variable on a probability space denoted $(\Xi, \mathcal{B}, \mathbb{P})$, $C \subseteq \mathbb{R}^n$ is a closed subdomain, and $\mathcal{R} : L^1(\Xi, \mathcal{B}, \mathbb{P}) \rightarrow \mathbb{R}$ is a *coherent risk measure* [1]. The canonical example of the objective function $F(x)$ is the expected value of f at x ; namely,

$$(1.2) \quad \mathbb{E}[f(x; \xi)] = \int_{\Xi} f(x; \xi) d\mathbb{P}(\xi).$$

In this situation, $\mathcal{R} = \mathbb{E}$ and we say that $F(x) = \mathbb{E}[f(x; \xi)]$ defines the expected risk at x .

With the expected value risk measure, $\mathcal{R} = \mathbb{E}$, the stochastic program (1.1) only seeks out the point $x = x^*$ which minimizes $f(x)$ on average. More general risk measures are often used when it is desirable to optimize for low probability events. The other risk measure considered in this work is the conditional value-at-risk (CVaR) [38, 39]. The CVaR at confidence level $\beta \in (0, 1)$, denoted CVaR_{β} , is a well-established decision-making tool in finance [31, 44] and is becoming increasingly prominent in engineering [14, 15, 29, 30, 41, 51]. In this work, stochastic programs featuring the risk measure $\mathcal{R} = \mathbb{E}$ are referred to as *risk-neutral*, meanwhile, those involving the risk measure $\mathcal{R} = \text{CVaR}_{\beta}$, are referred to as *risk-averse*.

*Submitted to the editors September 30, 2021.

Funding: This project received funding from the European Union's Horizon 2020 research and innovation programme under grant agreement No. 800898 as well as partial support from the German Research Foundation by grant WO671/11-1. In addition, much of the manuscript was written while the second author was in residence at the Institute for Computational and Experimental Research in Mathematics (ICERM) in Providence, RI, during the Advances in Computational Relativity program, supported by the National Science Foundation under Grant No. DMS-1439786. The first author gratefully acknowledges support from the International Research Training Group IGDK, funded by the German Science Foundation (DFG) and the Austrian ScienceFund (FWF).

[†]Mathematics and Cybernetics, SINTEF Digital, Strindvegen 4, 7034 Trondheim, NO (florian.beiser@sintef.no)

[‡]Lawrence Livermore National Laboratory, Center for Applied Scientific Computing, 7000 East Avenue, Livermore, CA 94550, USA (keith10@llnl.gov)

[§]School of Mathematical and Computer Sciences, Department of Actuarial Mathematics and Statistics, Heriot-Watt University, Edinburgh Campus, EH14 4AS, Edinburgh, UK (su2004@hw.ac.uk)

[¶]Chair for Numerical Mathematics, Department of Mathematics, Technical University of Munich, Boltzmannstraße 3, 80333 Munich, DE (wohlmuth@ma.tum.de)

In many practical problems, the integral in (1.2) cannot be computed directly because the space Ξ is high-dimensional or the measure \mathbb{P} is unknown [11, 28]. One common approach to approximate the integral is to draw a set of i.i.d. samples $S = \{\xi_i\}$, $i = 1, \dots, N$, of the random variable ξ and substitute $F(x)$ with the following empirical estimate of the expected risk:

$$(1.3) \quad F_S(x) = \frac{1}{N} \sum_{i=1}^N f(x; \xi_i).$$

When the sample set S is fixed, stochastic optimization methods which employ this type of approximation of the objective function are commonly referred to as sample average approximation methods [28, 43, 44]. In this paper, the set S will be determined *adaptively*.

In order to reduce the cost of optimization, we propose a sampling strategy which adaptively balances the algorithm’s sampling error and optimization error throughout the entire optimization process. The strategy works by updating the size of the sample set $S = S_k$ together with the point $x = x_k$, at each iteration k . This leads to robust and practical methods which can treat contemporary stochastic optimization problems more efficiently.

1.1. Literature review and motivation. There are many articles on stochastic optimization methods with dynamic sample sizes [8–13, 18, 22, 25, 27, 34, 35, 42, 43]. Nevertheless, very few of these works consider constrained optimization problems or risk-averse settings in detail [43]; the majority of the present literature focuses on unconstrained stochastic programs, such as those commonly found in machine learning. One notable exception is the recent contribution by Xie et al. [49, 50], which builds off an earlier version of this work and generalizes our treatment of deterministic constraints to a composite optimization setting of importance in some machine learning applications. Many contemporary methods follow from *a priori* error analysis, leading to prescribed growth in the sample size [9, 22, 43], ours does not. Instead, we choose to estimate the correct sample size *a posteriori* and update it adaptively.

Our work has a great deal in common with the adaptive sampling approaches taken in [8, 10, 12]. In order to highlight the primary similarities, we note that in our approach to (stochastic) projected gradient descent (Subsections 2.2 and 2.3 and Section 3), we arrive at a condition similar to the “norm test” introduced for unconstrained optimization in [12].¹ A similar test also appears in our sequential quadratic programming (SQP) algorithm (Section 4), where it could also be accompanied by two other conditions similar to the “inner product test” and the “orthogonality test”, respectively, first proposed in [8].

This work arose from a need to develop efficient stochastic programming methods for large-scale decision-making problems; especially in engineering design, where oversampling is extremely costly [23, 26, 27, 45, 52]. It is well-established that the expected risk (1.2) is often unsuitable to predict immediate and long-term performance, manufacturing and maintenance costs, system response, levels of damage, and numerous other quantities of interest [28–30, 37]. Therefore, today’s industrial problems are made even more challenging because they typically require a risk-averse formulation.

1.2. Layout. Apart from the expected value operator \mathbb{E} , the conditional value-at-risk is the only risk measure we consider in detail. It is well-known that this risk measure can be reformulated as a separate optimization problem involving \mathbb{E} ; cf. [38, 39] and Section 5. This observation informs the layout of the paper by allowing us to first focus on the case $\mathcal{R} = \mathbb{E}$ and then deal with the treatment of risk-averse problems in the later sections. A large family of other important risk measures have a similar reformulation involving \mathbb{E} [30, 40], which leads

¹The words “norm test” are not actually used in [12], but recent works by the authors of [12] have adopted this terminology; see, e.g., [8, 50].

us to conclude that there is little loss of generality in treating (1.1) in this incremental and case-specific way.

In Section 2, we use the expected risk problem to introduce basic adaptive sampling principles for stochastic projected gradient descent (SPGD) and theoretical conditions which imply convergence. We then use these conditions in Section 3 to propose a simple SPGD algorithm which solves the expected risk problem with convex constraints. In Section 4, we generalize this algorithm using SQP principles and arrive at a new algorithm appropriate for an important class of problems with non-convex constraints. In Section 5, we present two ways in which these algorithms may be extended to handle risk-averse problems. Here, we focus on the CVaR risk measure and state consequences for other important risk measures only in passing. Section 6 is dedicated to in-depth numerical studies which test the efficacy of our adaptive sampling method in its various forms. The paper closes with a short summary of results.

2. Adaptive sampling with convex constraints. In this and the two following sections, we only consider $\mathcal{R} = \mathbb{E}$. This setting allows (1.1) to be rewritten as

$$(2.1) \quad \min_{x \in C} \left\{ F(x) = \mathbb{E}[f(x; \xi)] \right\}.$$

For the time being, we also assume that $C \subseteq \mathbb{R}^n$ is convex. To treat this problem, we propose a projected gradient descent algorithm and sufficient conditions on the sample sets S_k , which guarantee that it is a descent method in expectation.

2.1. Preliminaries and notation. Let $\nabla F(x)$ denote the gradient of F at x and let $\langle \cdot, \cdot \rangle$ denote the ℓ^2 inner product on vectors in \mathbb{R}^n . It is well-known (see, e.g., [32]) that if F is both convex and continuously differentiable, then x^* is a solution of (2.1) if and only if

$$(2.2) \quad \langle \nabla F(x^*), x - x^* \rangle \geq 0$$

for all $x \in C$.

When $C = \mathbb{R}^n$, one may use the stochastic gradient descent algorithm, $x_{k+1} = x_k - \alpha \nabla F_{S_k}(x_k)$, to uncover locally optimal solutions of (2.1); cf. [8, 12]. Here, $\alpha > 0$ is a step-length parameter and $\nabla F_{S_k}(x_k)$ denotes the gradient of the sample average defined in (1.3) with an iteration-dependent sample set $S = S_k$. When the convex set $C \neq \mathbb{R}^n$, the analogue of this approach is the stochastic projected gradient descent (SPGD) algorithm; $y_{k+1} = x_k - \alpha \nabla F_{S_k}(x_k)$, $x_{k+1} = \arg \min_{x \in C} \|y_{k+1} - x\|^2$, where $\|\cdot\|$ denotes the Euclidean norm. Equivalently [32], we write

$$(2.3) \quad x_{k+1} = \arg \min_{x \in C} \left\{ F_{S_k}(x_k) + \langle \nabla F_{S_k}(x_k), x - x_k \rangle + \frac{1}{2\alpha} \|x - x_k\|^2 \right\}.$$

We will write $\mathbb{E}_k[\cdot]$ to denote the expected value operator (1.2), given x_k . With this notation, quantities such as $\mathbb{E}_k[F(x_{k+1})]$ are well-defined because x_{k+1} depends only on the random variable ξ through (1.3) and (2.3). We will also assume that S_k , for each k , is a set of i.i.d. samples, independent of each previous set S_0, S_1, \dots, S_{k-1} . With this assumption, $\nabla F_{S_k}(x_k)$ forms a unbiased estimator for the gradient at x_k , namely,

$$(2.4) \quad \mathbb{E}_k[\nabla F_{S_k}(x_k)] = \nabla F(x_k).$$

When we wish to analyze the *total expectation* of an iteration-dependent quantity, say $\mathbb{E}[F(x_k)]$, we note that it is completely determined by the joint distribution of samples in S_0, S_1, \dots, S_{k-1} . For this reason, we have the identity [11]

$$(2.5) \quad \mathbb{E}[F(x_k)] = \mathbb{E}_0 \mathbb{E}_1 \cdots \mathbb{E}_{k-1}[F(x_k)].$$

In the sequel, it will also be convenient to assign symbols to certain terms in the equations above. First, we define the orthogonal projection onto C ,

$$P(y) = \arg \min_{x \in C} \|y - x\|^2.$$

Note that because C is convex, $P(y)$ is unique and non-expansive, namely,

$$(2.6) \quad \|P(x) - P(y)\|^2 \leq \langle x - y, P(x) - P(y) \rangle \leq \|x - y\|^2,$$

and generally it is *non-linear*. Next, we denote the projected gradient mapping, $Q : \mathbb{R}^n \rightarrow C$, as $Q(x) = P(x - \alpha \nabla F(x))$. Equivalently, one may write

$$(2.7) \quad Q(x) = \arg \min_{y \in C} \left\{ F(x) + \langle \nabla F(x), y - x \rangle + \frac{1}{2\alpha} \|y - x\|^2 \right\}.$$

The subsampled gradient map is then defined analogously to (2.7); namely,

$$(2.8) \quad Q_{S_k}(x) = \arg \min_{y \in C} \left\{ F_{S_k}(x) + \langle \nabla F_{S_k}(x), y - x \rangle + \frac{1}{2\alpha} \|y - x\|^2 \right\}.$$

With this notation in hand, one may note that $x_{k+1} = Q_{S_k}(x_k)$ by (2.3).

The reduced gradient, defined

$$R(x) = \alpha^{-1}(x - Q(x)),$$

is another important operator we will make judicious use of. The subsampled reduced gradient is likewise defined

$$R_{S_k}(x) = \alpha^{-1}(x - Q_{S_k}(x)).$$

Clearly, $x_{k+1} = x_k - \alpha R_{S_k}(x_k)$. Moreover, when $C = \mathbb{R}^n$, one may note that $R(x_k) = \nabla F(x_k)$ and $R_{S_k}(x_k) = \nabla F_{S_k}(x_k)$.

We may now formulate the first-order optimality condition for (2.1) as follows [32]:

If x^* is a minimizer of (2.1), then $Q(x^*) = x^*$ and $R(x^*) = 0$.

We may also state two lemmas based on [32], which will be useful later on. For reference, we say that F is L -smooth if

$$(2.9) \quad \|\nabla F(x) - \nabla F(y)\| \leq L\|x - y\|,$$

for all $x, y \in C$, and we say that F is μ -strongly convex if

$$(2.10) \quad F(y) \geq F(x) + \langle \nabla F(x), y - x \rangle + \frac{\mu}{2} \|y - x\|^2.$$

The proof of Lemma 2.1 can be found in [32, Corollary 2.2.4]. For the reader's convenience, we include the proof of Lemma 2.2.

LEMMA 2.1. *Assume that F is L -smooth and let $0 < \alpha \leq 1/L$. If F is convex, then the following inequality holds for all $x \in C$:*

$$(2.11) \quad F(Q(x)) - F(x) \leq -\frac{\alpha}{2} \|R(x)\|^2.$$

If, moreover, F is μ -strongly convex, then it also holds that

$$(2.12) \quad \frac{\mu}{2} \|x - x^*\|^2 + \frac{\alpha}{2} \|R(x)\|^2 \leq \langle R(x), x - x^* \rangle.$$

LEMMA 2.2. *Let F be L -smooth and let C be closed and convex. For all $y \in C$ and $z \in \mathbb{R}^n$, it holds that*

$$(2.13) \quad \langle R(z), y - Q(z) \rangle \leq \langle \nabla F(z), y - Q(z) \rangle.$$

Proof. Fix $z \in \mathbb{R}^n$ and consider $\phi(y) = F(z) + \langle \nabla F(z), y - z \rangle + \frac{1}{2\alpha} \|y - z\|^2$. Note that ϕ is both convex and continuously differentiable and that $\nabla \phi(y) = \nabla F(z) + \frac{1}{\alpha}(y - z)$. Therefore, following from the optimality condition (2.2) and the definition of $Q(\cdot)$ in (2.7), it holds that

$$\langle \nabla \phi(Q(z)), y - Q(z) \rangle = \langle \nabla F(z) - R(z), y - Q(z) \rangle \geq 0$$

for all $y \in C$. \square

2.2. Descent conditions. The goal of our adaptive sampling scheme is to balance sampling and optimization error. One way to strike this balance is through state-dependent conditions which ensure that $\mathbb{E}_k[F(x_{k+1})] \leq F(x_k)$. In Theorem 2.3, we show that it is sufficient that each sample set S_k satisfies only two idealized conditions. However, we note that these conditions require foreknowledge of the exact gradient at each iterate, x_k . (This detail is dealt with in Section 3.) The descent conditions are:

CONDITION 1. *Control of the norm of the reduced gradient:*

$$(2.14) \quad \mathbb{E}_k[\|R_{S_k}(x_k)\|^2] \leq (1 + \nu^2)\|R(x_k)\|^2,$$

for some fixed $\nu > 0$.

CONDITION 2. *Control of the bias in the projected gradient mapping:*

$$(2.15) \quad \|\mathbb{E}_k[Q_{S_k}(x_k) - Q(x_k)]\| \leq \frac{\gamma^2}{2}\|Q(x_k) - x_k\|^2,$$

for some fixed $\gamma > 0$.

THEOREM 2.3. *Assume that F is L -smooth (2.9) and that the sequence of iterates $\{x_k\}_{k=0}^\infty$ is contained in an open set over which $\|\nabla F(x)\|$ is bounded above by some constant $M > 0$. If S_k satisfies Conditions 1 and 2 and $\alpha \leq \frac{2}{M\gamma^2 + L(1 + \nu^2)}$, then*

$$\mathbb{E}_k[F(x_{k+1})] \leq F(x_k).$$

Proof. By standard arguments following from the L -smoothness of F [3], we have that

$$(2.16) \quad \begin{aligned} F(x_{k+1}) &\leq F(x_k) + \langle \nabla F(x_k), x_{k+1} - x_k \rangle + \frac{L}{2}\|x_{k+1} - x_k\|^2 \\ &= F(x_k) + \langle \nabla F(x_k), Q(x_k) - x_k \rangle + \langle \nabla F(x_k), E_{S_k}(x_k) \rangle + \frac{L}{2}\|x_{k+1} - x_k\|^2, \end{aligned}$$

where $E_{S_k}(x_k) = x_{k+1} - Q(x_k)$. Now, substituting $y = z = x_k$ into (2.13), we arrive at the identity

$$(2.17) \quad \langle \nabla F(x_k), Q(x_k) - x_k \rangle \leq -\langle R(x_k), x_k - Q(x_k) \rangle = -\frac{1}{\alpha}\|x_k - Q(x_k)\|^2.$$

Next, Condition 2 implies that

$$(2.18) \quad \mathbb{E}_k[\langle \nabla F(x_k), E_{S_k}(x_k) \rangle] \leq \|\nabla F(x_k)\| \|\mathbb{E}_k[E_{S_k}(x_k)]\| \leq \frac{M}{2}\gamma^2\|Q(x_k) - x_k\|^2.$$

Moreover, [Condition 1](#) implies that

$$(2.19) \quad \mathbb{E}_k[\|x_{k+1} - x_k\|^2] = \alpha^2 \mathbb{E}_k[\|R_{S_k}(x_k)\|^2] \leq \alpha^2(1+\nu^2)\|R(x_k)\|^2 = (1+\nu^2)\|Q(x_k) - x_k\|^2.$$

Combining [\(2.16\)](#)–[\(2.19\)](#), we arrive at

$$(2.20) \quad \mathbb{E}_k[F(x_{k+1})] - F(x_k) \leq -c\|Q(x_k) - x_k\|^2,$$

where $c = \frac{1}{\alpha} - \frac{L}{2}(1+\nu^2) - \frac{M}{2}\gamma^2$. Note that if $\alpha \leq \frac{2}{M\gamma^2 + L(1+\nu^2)}$, then the right-hand side of [\(2.20\)](#) is non-positive. \square

Although conditions [\(2.14\)](#) and [\(2.15\)](#) are simple to write out, it is unfortunately difficult to design practical algorithms which directly enforce them. For this reason, we turn to an alternative condition in the next subsection.

Remark 2.4. Inspecting the proof of [Theorem 2.3](#), in particular inequality [\(2.20\)](#), we see that if $\alpha \leq \frac{1}{M\gamma^2 + L(1+\nu^2)}$, then $c \geq \frac{1}{2\alpha}$. With this stronger condition, we may write

$$\mathbb{E}_k[F(x_{k+1})] - F(x_k) \leq -\frac{\alpha}{2}\|R(x_k)\|^2,$$

which is similar to [\(2.11\)](#). Similar bounds on the step size α will appear again. To simplify these expressions, we adopt the notation

$$(2.21) \quad \tilde{L} = M\gamma^2 + L(1+\nu^2).$$

2.3. Alternative condition. Let us focus on the bias condition given by [\(2.15\)](#). Further light can be shed on it if we assume that the boundary of the constraint set C is smooth. In this setting, we may write out a first-order Taylor expansion for $Q_{S_k}(x) = P(x - \alpha\nabla F(x) - \alpha(\nabla F_{S_k}(x) - \nabla F(x)))$ as follows:

$$(2.22) \quad \begin{aligned} Q_{S_k}(x) &= Q(x) - \alpha\langle \nabla P(x - \alpha\nabla F(x)), \nabla F_{S_k}(x) - \nabla F(x) \rangle \\ &\quad + \mathcal{O}(\alpha^2\|\nabla F_{S_k}(x) - \nabla F(x)\|^2). \end{aligned}$$

Therefore, because $\mathbb{E}_k[\nabla F_{S_k}(x) - \nabla F(x)] = 0$, by [\(2.4\)](#), we arrive at the order estimate

$$(2.23) \quad \|\mathbb{E}_k[Q_{S_k}(x_k) - Q(x_k)]\| = \mathcal{O}(\alpha^2\mathbb{E}_k[\|\nabla F_{S_k}(x_k) - \nabla F(x_k)\|^2]).$$

If we notice that $\|Q(x_k) - x_k\|^2 = \alpha^2\|R(x_k)\|^2$, it now seems very appealing to replace [Condition 2](#) by the following alternative condition, which delivers a probabilistic threshold on $\nabla F_{S_k}(x_k)$ lying within a ball around $\nabla F(x_k)$:

CONDITION 3. *Control of the error in the full gradient by the norm of the reduced gradient:*

$$(2.24) \quad \mathbb{E}_k[\|\nabla F_{S_k}(x_k) - \nabla F(x_k)\|^2] \leq \theta^2\|R(x_k)\|^2,$$

for some fixed $\theta > 0$.

[Condition 3](#) is a direct generalization of the so-called “norm test” for stochastic gradient descent proposed in [\[12\]](#). Although [Condition 3](#) also requires unattainable foreknowledge of the exact gradient, it is possible to design a practical algorithm around it. This aspect is discussed in the next section. Before then, however, we establish a number of theoretical properties related to the conditions above.

We finish this subsection by showing that under certain assumptions, [Condition 3](#) implies [Condition 1](#) and [Condition 3](#) also implies [Condition 2](#). This observation is encapsulated in [Theorem 2.5](#). The remainder of this section is devoting to analyzing the convergence of the stochastic projected gradient descent algorithm [\(2.3\)](#) when either [Condition 1](#), [2](#), or [3](#) is enforced.

THEOREM 2.5. *Condition 3 implies Condition 1 with $\nu = \sqrt{2\theta + \theta^2}$. If, in addition,*

$$(2.25) \quad \mathbb{E}[\|\nabla f(x; \xi) - \nabla F(x)\|^2] < \infty$$

for all $x \in C$, $P(\cdot) : \mathbb{R}^n \rightarrow C$ is twice differentiable, and $|S_k|$ is sufficiently large, then Condition 3 implies Condition 2 with some $\gamma \propto \theta$.

Proof. To prove the first statement, it is important that we recall that $P(\cdot)$ is non-expansive (2.6). Due to this property, we have

$$(2.26) \quad \begin{aligned} \|R_{S_k}(x_k) - R(x_k)\| &= \frac{1}{\alpha} \|P(x_k - \alpha \nabla F_{S_k}(x_k)) - P(x_k - \alpha \nabla F(x_k))\| \\ &\leq \|\nabla F_{S_k}(x_k) - \nabla F(x_k)\|. \end{aligned}$$

Therefore, by (2.24),

$$(2.27) \quad \|\mathbb{E}_k[R_{S_k}(x_k) - R(x_k)]\| \leq (\mathbb{E}_k[\|R_{S_k}(x_k) - R(x_k)\|^2])^{1/2} \leq \theta \|R(x_k)\|.$$

Likewise,

$$(2.28) \quad \begin{aligned} \mathbb{E}_k[\|R_{S_k}(x_k)\|^2] &= \|R(x_k)\|^2 + 2\langle R(x_k), \mathbb{E}_k[R_{S_k}(x_k) - R(x_k)] \rangle + \mathbb{E}_k[\|R_{S_k}(x_k) - R(x_k)\|^2] \\ &\leq \|R(x_k)\|^2 + 2\|R(x_k)\| \|\mathbb{E}_k[R_{S_k}(x_k) - R(x_k)]\| + \mathbb{E}_k[\|R_{S_k}(x_k) - R(x_k)\|^2] \\ &\leq \|R(x_k)\|^2 + 2\theta \|R(x_k)\|^2 + \theta^2 \|R(x_k)\|^2 \\ &\leq (1 + \theta)^2 \|R(x_k)\|^2. \end{aligned}$$

In other words, Condition 1 holds with $\nu = \sqrt{2\theta + \theta^2}$.

To prove the second statement, we must argue that $\mathbb{E}_k[\|\nabla F_{S_k}(x_k) - \nabla F(x_k)\|^2] \rightarrow 0$ as $|S_k| \rightarrow \infty$. Indeed, notice that

$$(2.29) \quad \mathbb{E}_k[\|\nabla F_{S_k}(x_k) - \nabla F(x_k)\|^2] = \frac{\mathbb{E}_k[\|\nabla f(x_k; \xi) - \nabla F(x_k)\|^2]}{|S_k|} \rightarrow 0,$$

since the numerator is independent of $|S_k|$ by (2.25). Now, immediately following from (2.23), there exists some step-size independent constant, say $c \geq 0$, such that

$$\|\mathbb{E}_k[Q_{S_k}(x_k) - Q(x_k)]\| \leq c\alpha^2 \mathbb{E}_k[\|\nabla F_{S_k}(x_k) - \nabla F(x_k)\|^2],$$

for all sufficiently large $|S_k|$. Invoking Condition 3, we have

$$\|\mathbb{E}_k[Q_{S_k}(x_k) - Q(x_k)]\| \leq c\theta^2 \alpha^2 \|R(x_k)\|^2 = c\theta^2 \|Q(x_k) - x_k\|^2,$$

and thus Condition 2 holds with $\gamma = \theta\sqrt{2c}$. This completes the proof. \square

Remark 2.6. The regularity assumption made in this subsection may appear rather restrictive. Fortunately, however, the practical algorithm which Condition 3 leads to (i.e., Algorithm 1) appears to perform remarkably well, even when this assumption is clearly violated; cf. Section 6.

Remark 2.7. One may notice that if C is affine, then the second order term in (2.22) actually disappears and Condition 2 is satisfied trivially. We will argue in Section 4 that this special setting permits us to propose other alternative conditions which are weaker than Condition 3.

2.4. Convergence. Convergence of SPGD can be shown under a variety of assumptions involving [Conditions 1–3](#). We begin this subsection by showing that [Condition 3](#) implies q -linear convergence when F is strongly convex.

THEOREM 2.8 (Strongly convex objective). *Let F be both L -smooth [\(2.9\)](#) and μ -strongly convex [\(2.10\)](#) and let C be both convex and closed. Moreover, let the infinite sequence $\{x_k\}_{k=0}^\infty$ be generated by [\(2.3\)](#), with*

$$\alpha < \frac{1}{L}$$

and each S_k satisfying [Condition 3](#). Then, for all sufficiently small $\theta > 0$, x_k converges q -linearly in expectation; i.e.,

$$\mathbb{E}[\|x_{k+1} - x^*\|] \leq \rho^k \|x_0 - x^*\|,$$

for some $\rho \in [0, 1)$, where $x^* = \arg \min_{x \in C} F(x)$.

Proof. By [\(2.5\)](#), it is sufficient to show that $\mathbb{E}_k[\|x_{k+1} - x^*\|] \leq \rho \|x_k - x^*\|$, for every k . To this end, denote $E_{S_k}(x_k) = Q_{S_k}(x_k) - Q(x_k)$ and observe that

$$\begin{aligned} (\mathbb{E}_k[\|x_{k+1} - x^*\|])^2 &\leq \mathbb{E}_k[\|x_{k+1} - x^*\|^2] = \mathbb{E}_k[\|x_k - \alpha R_{S_k}(x_k) - x^*\|^2] \\ &= \|x_k - x^*\|^2 + \alpha^2 \mathbb{E}_k[\|R_{S_k}(x_k)\|^2] - 2\alpha \mathbb{E}_k[\langle R_{S_k}(x_k), x_k - x^* \rangle] \\ &= \|x_k - x^*\|^2 + \alpha^2 \mathbb{E}_k[\|R_{S_k}(x_k)\|^2] - 2\alpha \langle R(x_k), x_k - x^* \rangle \\ &\quad + 2 \langle \mathbb{E}_k[E_{S_k}(x_k)], x_k - x^* \rangle. \end{aligned}$$

Now, by [Theorem 2.5](#), we have

$$\mathbb{E}_k[\|R_{S_k}(x_k)\|^2] \leq (1 + \nu^2) \|R(x_k)\|^2,$$

with $\nu^2 = 2\theta + \theta^2$. Furthermore, by [\(2.12\)](#), we have

$$-2\alpha \langle R(x_k), x_k - x^* \rangle \leq -\mu\alpha \|x_k - x^*\|^2 - \alpha^2 \|R(x_k)\|^2,$$

and, by [\(2.27\)](#), we have

$$2 \langle \mathbb{E}_k[E_{S_k}(x_k)], x_k - x^* \rangle \leq 2 \|\mathbb{E}_k[E_{S_k}(x_k)]\| \|x_k - x^*\| \leq 2\alpha\theta \|R(x_k)\| \|x_k - x^*\|.$$

Combining each of these bounds, we find that

$$(2.30) \quad \mathbb{E}_k[\|x_{k+1} - x^*\|^2] \leq (1 - \mu\alpha) \|x_k - x^*\|^2 + 2\alpha\theta \|R(x_k)\| \|x_k - x^*\| + \alpha^2(2\theta + \theta^2) \|R(x_k)\|^2.$$

Invoking [\(2.12\)](#) a second time, along with the Cauchy–Schwarz inequality, yields

$$\frac{\mu}{2} \|x_k - x^*\|^2 + \frac{\alpha}{2} \|R(x_k)\|^2 \leq \|R(x_k)\| \|x_k - x^*\|.$$

Note that $\mu \leq L$ and so $\alpha\mu < \mu/L \leq 1$. Moreover, the two roots of the equation $\mu a^2 + \alpha b^2 = 2ab$ are $b = (1 \pm \sqrt{1 - \alpha\mu})a/\alpha$. Thus, it follows that

$$(2.31) \quad (1 - \sqrt{1 - \alpha\mu}) \|x_k - x^*\| \leq \alpha \|R(x_k)\| \leq (1 + \sqrt{1 - \alpha\mu}) \|x_k - x^*\|.$$

We may now replace every $\alpha \|R(x_k)\|$ factor in [\(2.30\)](#) by the upper bound given in [\(2.31\)](#). A straightforward simplification of the resulting inequality yields

$$\mathbb{E}_k[\|x_{k+1} - x^*\|^2] \leq \left(1 + 2(1 + \sqrt{1 - \alpha\mu})(3\theta + \theta^2) - (1 + \theta)^2 \mu\alpha\right) \|x_k - x^*\|^2.$$

Finally, note that if θ is chosen sufficiently small, then

$$\rho^2 := 1 + 2(1 + \sqrt{1 - \alpha\mu})(3\theta + \theta^2) - (1 + \theta)^2\mu\alpha \leq 1 + 4(3\theta + \theta^2) - \mu\alpha < 1,$$

as necessary. \square

Conditions 1 and **2** can also be shown to imply convergence. In the following theorem, we show that it is possible to arrive at a sublinear convergence rate with a general convex objective function F .

THEOREM 2.9 (General convex objective). *Assume that F is L -smooth (2.9) and C is convex and closed and that the sequence of iterates $\{x_k\}_{k=0}^\infty$ is contained in an bounded open set D over which $\|\nabla F(x)\|$ is bounded above by some constant $M > 0$. Moreover, assume that*

$$\tilde{L}\alpha + \nu^2 + \gamma^2 \text{diam}(D) < 1$$

where each S_k satisfies **Conditions 1** and **2**. Then, for every any positive integer T ,

$$\mathbb{E}[F(x_T)] - F^* \leq \frac{1}{2\alpha T} \|x_0 - x^*\|^2,$$

where F^* is the optimal objective function value and $x^* \in \{x : x = \arg \min_{x \in C} F(x)\}$.

Proof. Notice that

$$\|x_{k+1} - x_k\|^2 + \|x_k - x^*\|^2 - \|x_{k+1} - x^*\|^2 = 2\langle x_k - x_{k+1}, x_k - x^* \rangle.$$

Using the identity $x_k - x_{k+1} = \alpha R_{S_k}(x_k)$ and rearranging terms, we arrive at

$$\|x_{k+1} - x^*\|^2 - \|x_k - x^*\|^2 = 2\alpha \langle R(x_k), x^* - x_k \rangle - 2\langle E_{S_k}(x_k), x^* - x_k \rangle + \alpha^2 \|R_{S_k}(x_k)\|^2,$$

where $E_{S_k}(x_k) = x_{k+1} - Q(x_k)$. Taking the expected value of both sides, we find

$$\begin{aligned} \mathbb{E}_k[\|x_{k+1} - x^*\|^2] - \|x_k - x^*\|^2 &\leq 2\alpha \langle R(x_k), x^* - x_k \rangle + 2\|\mathbb{E}_k[E_{S_k}(x_k)]\| \|x^* - x_k\| + \alpha^2 \mathbb{E}_k[\|R_{S_k}(x_k)\|^2] \\ (2.32) \quad &\leq 2\alpha \langle R(x_k), x^* - x_k \rangle + \alpha^2 (1 + \nu^2 + \gamma^2 \|x^* - x_k\|) \|R(x_k)\|^2. \end{aligned}$$

By setting $y = x^*$ and $z = x_k$ in **Lemma 2.2**, we may write

$$\langle R(x_k), x^* - x_k \rangle + \langle R(x_k), x_k - Q(x_k) \rangle \leq \langle \nabla F(x_k), x^* - x_k \rangle + \langle \nabla F(x_k), x_k - Q(x_k) \rangle.$$

Note that $\langle R(x_k), x_k - Q(x_k) \rangle = \alpha \|R(x_k)\|^2$, by definition, and $\langle \nabla F(x_k), x^* - x_k \rangle \leq F^* - F(x_k)$, by convexity. By standard arguments following from the L -smoothness of F [3], we have that

$$\begin{aligned} \langle \nabla F(x_k), x_k - Q(x_k) \rangle &= \langle \nabla F(x_k), x_k - x_{k+1} \rangle + \langle \nabla F(x_k), x_{k+1} - Q(x_k) \rangle \\ &\leq F(x_k) - F(x_{k+1}) + \frac{L}{2} \|x_{k+1} - x_k\|^2 + \langle \nabla F(x_k), x_{k+1} - Q(x_k) \rangle. \end{aligned}$$

Taking the conditional expectation of both sides yields

$$\begin{aligned} \langle \nabla F(x_k), x_k - Q(x_k) \rangle &\leq F(x_k) - \mathbb{E}_k[F(x_{k+1})] + \frac{L}{2} \mathbb{E}_k[\|x_{k+1} - x_k\|^2] + \langle \nabla F(x_k), \mathbb{E}_k[x_{k+1} - Q(x_k)] \rangle \\ &\leq F(x_k) - F(x_{k+1}) + \frac{\alpha^2}{2} (L(1 + \nu^2) + M\gamma^2) \|R(x_k)\|^2. \end{aligned}$$

Therefore,

$$\begin{aligned}
 \langle R(x_k), x^* - x_k \rangle &\leq \langle \nabla F(x_k), x^* - x_k \rangle + \langle \nabla F(x_k), x_k - Q(x_k) \rangle - \langle R(x_k), x_k - Q(x_k) \rangle \\
 &\leq (F^* - F(x_k)) + \left(F(x_k) - F(x_{k+1}) + \frac{\tilde{L}}{2} \alpha^2 \|R(x_k)\|^2 \right) - \alpha \|R(x_k)\|^2 \\
 (2.33) \quad &= F^* - F(x_{k+1}) + \alpha \left(\frac{\tilde{L}\alpha}{2} - 1 \right) \|R(x_k)\|^2.
 \end{aligned}$$

Finally, collecting together (2.32) and (2.33), we find

$$\begin{aligned}
 \mathbb{E}_k[\|x_{k+1} - x^*\|^2] - \|x_k - x^*\|^2 &\leq 2\alpha(F^* - F(x_{k+1})) + \alpha^2(\tilde{L}\alpha + \nu^2 + \gamma^2\|x^* - x_k\| - 1)\|R(x_k)\|^2 \\
 &\leq 2\alpha(F^* - F(x_{k+1})),
 \end{aligned}$$

where the second inequality follows from the bounds on α , ν , and γ made in the theorem statement. We can now write

$$\mathbb{E}[F(x_{k+1})] - F^* \leq \frac{1}{2\alpha} \left(\mathbb{E}[\|x_k - x^*\|^2] - \mathbb{E}[\|x_{k+1} - x^*\|^2] \right),$$

which, after invoking Theorem 2.3, delivers the bound

$$\begin{aligned}
 \mathbb{E}[F(x_T)] - F^* &\leq \sum_{k=0}^{T-1} \frac{1}{T} (\mathbb{E}[F(x_{k+1})] - F^*) \\
 &\leq \frac{1}{2\alpha T} \left(\mathbb{E}[\|x_0 - x^*\|^2] - \mathbb{E}[\|x_T - x^*\|^2] \right) \\
 &\leq \frac{1}{2\alpha T} \mathbb{E}[\|x_0 - x^*\|^2]. \quad \square
 \end{aligned}$$

The following theorem shows an even weaker version of convergence which requires only the same mild assumptions as were made in Theorem 2.3. In particular, it shows that the sequence of reduced gradients $\{R(x_k)\}$ converges to zero in expectation. Therefore, every limit point x^* of the sequence x_k is stationary; i.e., $Q(x^*) = x^*$. This theorem also establishes a global sublinear rate of convergence of the smallest reduced gradients.

THEOREM 2.10 (Non-convex objective). *Under the assumptions of Theorem 2.3, it holds that*

$$\lim_{k \rightarrow \infty} \mathbb{E}[\|R(x_k)\|^2] = \lim_{k \rightarrow \infty} \mathbb{E}[\|Q(x_k) - x_k\|^2] = 0.$$

Moreover, for any positive integer T ,

$$\min_{0 \leq k \leq T-1} \mathbb{E}[\|R(x_k)\|^2] \leq \frac{1}{c\alpha^2 T} (F(x_0) - F_{\min}),$$

where $c = \frac{1}{\alpha} - \frac{\tilde{L}}{2} > 0$ and F_{\min} is a finite lower bound on F in C .

Proof. Begin by taking the total expected value of both sides of (2.20) and rewriting the result as

$$(2.34) \quad \mathbb{E}[\|R(x_k)\|^2] = \frac{1}{\alpha^2} \mathbb{E}[\|Q(x_k) - x_k\|^2] \leq \frac{1}{c\alpha^2} (\mathbb{E}[F(x_k)] - \mathbb{E}[F(x_{k+1})]).$$

It follows from the step size assumption in [Theorem 2.3](#) that $c > 0$. Therefore, summing both sides of [\(2.34\)](#) delivers

$$\sum_{k=0}^{T-1} \mathbb{E}[\|R(x_k)\|^2] \leq \frac{1}{c\alpha^2} (\mathbb{E}[F(x_0)] - \mathbb{E}[F(x_T)]) \leq \frac{1}{c\alpha^2} (F(x_0) - F_{\min}).$$

Since this sum of T positive terms is bounded from above by a constant independent of T , the first statement follows. Moreover, notice that

$$\min_{0 \leq k \leq T-1} \mathbb{E}[\|R(x_k)\|^2] \leq \frac{1}{T} \sum_{k=0}^{T-1} \mathbb{E}[\|R(x_k)\|^2] \leq \frac{1}{c\alpha^2 T} (F(x_0) - F_{\min}).$$

This completes the proof. \square

Remark 2.11. [Theorems 2.9](#) and [2.10](#) apply to SPGD satisfying [Conditions 1](#) and [2](#) at each iteration. However, by [Theorem 2.5](#), they also apply to SPGD satisfying [Condition 3](#) when the boundary of C is sufficiently smooth.

3. A practical algorithm. In this section, we develop a practical SPGD algorithm based on [Condition 3](#). In order to test whether this condition is satisfied, we introduce an approximation of the true gradient $\nabla F(x_k)$ and the risk measure $\mathbb{E}[\cdot]$. We begin by recalling [\(2.29\)](#), which allows us to rewrite [\(2.24\)](#) as

$$\frac{\mathbb{E}_k[\|\nabla f(x_k; \xi) - \nabla F(x_k)\|^2]}{|S_k|} \leq \theta^2 \|R(x_k)\|^2.$$

We then approximate the true gradient $\nabla F(x_k)$ by the sample average gradient $\nabla F_{S_k}(x_k)$, used previously. Likewise, we approximate of the conditional expected value $\mathbb{E}_k[\cdot]$ by a sample average. Altogether, we propose the following practical test to check [Condition 3](#):

TEST 1 (Approximation of [Condition 3](#)). *Approximate control of the error in the full gradient by the norm of the reduced gradient:*

$$(3.1) \quad \frac{1}{|S_k| - 1} \frac{\sum_{\xi \in S_k} \|\nabla f(x_k; \xi) - \nabla F_{S_k}(x_k)\|^2}{|S_k|} \leq \theta^2 \|R_{S_k}(x_k)\|^2,$$

for some fixed $\theta > 0$.

In [\(3.1\)](#), we have used the factor $\frac{1}{|S_k| - 1}$ instead of $\frac{1}{|S_k|}$ so that the left-hand side becomes an unbiased estimator for $\mathbb{E}_k[\|\nabla F_{S_k}(x_k) - \nabla F(x_k)\|^2]$.

In order to construct a set S_k satisfying [\(3.1\)](#), one may envision starting with a sample set S_k of a minimal size, say $|S_k| = |S_0|$, and simply adding samples until [\(3.1\)](#) holds. This strategy, however, would be too expensive to be practical as it would require recomputing $R_{S_k}(x_k)$ each time the set S_k is updated. Because of the expense of applying $P(\cdot)$, we choose to only consider strategies which involve computing $R_{S_k}(x_k)$ once each iteration.

One natural thing to consider is to use [\(3.1\)](#) to predict the correct size of the *upcoming* sample set S_{k+1} . Such a strategy may work as follows. Begin by dividing the left-hand side of [\(3.1\)](#) by $\theta^2 \|R_{S_k}(x_k)\|^2$ and, in turn, define the new quantity

$$\rho = \frac{\sum_{\xi \in S_k} \|\nabla f(x_k; \xi) - \nabla F_{S_k}(x_k)\|^2}{\theta^2 (|S_k| - 1) |S_k| \|R_{S_k}(x_k)\|^2}.$$

When [\(3.1\)](#) is satisfied, we clearly have $\rho \leq 1$, and we simply keep the sample size fixed; that is, $|S_{k+1}| = |S_k|$. On the other hand, if the test fails, $\rho > 1$ is used to increase the sample size via

the update rule

$$(3.2) \quad |S_{k+1}| = \lceil \rho |S_k| \rceil.$$

The procedure above leads to the following algorithm:

Algorithm 1: SPGD adaptive sampling algorithm for convex stochastic programs

input : x_0 , step size $\alpha > 0$, initial sample set S_0 , sampling rate parameter $\theta > 0$

Set $k \leftarrow 0$.

repeat

 Update $x_{k+1} = Q_{S_k}(x_k)$.

if *Test 1 is not satisfied* **then**

 Construct S_{k+1} obeying (3.2).

else

 Construct S_{k+1} satisfying $|S_{k+1}| = |S_k|$.

 Set $k \leftarrow k + 1$.

until *until a convergence test is satisfied*

4. Treatment of non-convex constraints. Up to this point, the convexity of C has been critical. In fact, it is required to even uniquely define several of the operators introduced in Subsection 2.1. Nevertheless, many optimization problems involve non-convex constraints and some of the ideas introduced above can still be used in that setting. We give one example and leave its generalizations for future study.

Assume that C is the level set of a smooth function $G : \mathbb{R}^n \rightarrow \mathbb{R}$. In this case, we may rewrite (2.1) as

$$\min_{x \in \mathbb{R}^n} \left\{ F(x) = \mathbb{E}[f(x; \xi)] \quad \text{subject to } G(x) = 0 \right\}.$$

This problem can be solved with sequential quadratic programming (SQP) principles; see, e.g., [24, 33, 46]. In its most basic form, we seek the optimum

$$(4.1) \quad d_{S_k} = \arg \min_{d \in \mathbb{R}^n} \langle \nabla F_{S_k}(x_k), d \rangle + \frac{1}{2\alpha} \|d\|^2 \quad \text{subject to } \langle \nabla G(x_k), d \rangle + G(x_k) = 0,$$

and update the solution $x_k \mapsto x_k + d_{S_k}$.

The parameter $\alpha > 0$ in (4.1) plays a similar role as in the previous sections. Indeed, a straightforward computation shows that the solution to (4.1) is precisely $d_{S_k} = -\alpha R_{S_k}(x_k)$ when the affine set $C_k = \{y \in \mathbb{R}^n : \langle \nabla G(x_k), y - x_k \rangle + G(x_k) = 0\}$ is substituted for C in definition (2.8). This observation establishes a connection between the preceding analysis and the treatment of non-convex constraints via SQP methods. Throughout the rest of this section, when we refer to $R_{S_k}(x_k)$ or $R(x_k)$, we assume that $C = C_k$ at each iteration k .

Now, as stated in Remark 2.7, Condition 2 is trivially satisfied when C is affine. This clearly happens to be the case in (4.1). It is interesting to note that an affine constraint set makes it possible to propose alternatives to Condition 3 which are less restrictive on the size of the sample set S_k . One possibility is to propose a probabilistic threshold on $R_{S_k}(x_k)$ lying within a ball around $R(x_k)$. This may be written as follows:

CONDITION 4. *Control of the error in the reduced gradient by the norm of the reduced gradient:*

$$\mathbb{E}_k [\|R_{S_k}(x_k) - R(x_k)\|^2] \leq \theta^2 \|R(x_k)\|^2,$$

for some fixed $\theta > 0$.

We note that [Condition 4](#) is weaker than [Condition 3](#) because of [\(2.26\)](#). Nevertheless, one can easily proceed from [\(2.28\)](#) to show that [Condition 4](#) implies [Condition 1](#).

In order to derive a practical SQP algorithm with adaptive sampling, let us define

$$(4.2) \quad d(x_k; \xi) = \arg \min_{d \in \mathbb{R}^n} \langle \nabla f(x_k; \xi), d \rangle + \frac{1}{2\alpha} \|d\|^2 \quad \text{subject to } \langle \nabla G(x_k), d \rangle + G(x_k) = 0$$

and, accordingly, $R(x_k; \xi) = -\frac{1}{\alpha} d(x_k; \xi)$. We then propose the following test which may be used to check [Condition 4](#).

TEST 2 (Approximation of [Condition 4](#)). *Approximate control of the error in the reduced gradient by the norm of the reduced gradient:*

$$\frac{1}{|S_k| - 1} \frac{\sum_{\xi \in S_k} \|R(x_k; \xi) - R_{S_k}(x_k)\|^2}{|S_k|} \leq \theta^2 \|R_{S_k}(x_k)\|^2,$$

for some fixed $\theta > 0$.

In the following algorithm involving [Test 2](#), note that the sample set S_k is updated *before* progressing to the next iteration. This is a desirable choice when collecting samples is more expensive than solving [\(4.1\)](#) or [\(4.2\)](#), which happens to be the case in the engineering example considered in [Subsection 6.3](#).

Algorithm 2: SQP adaptive sampling algorithm for stochastic programs with functional equality constraints

input: x_0 , step size $\alpha > 0$, initial sample set S_0 , constant $\theta > 0$

Set $k \leftarrow 0$.

repeat

if [Test 2](#) is satisfied **then**

 Update $x_{k+1} = x_k + d_{S_k}$.

 Set $k \leftarrow k + 1$.

 Construct S_k satisfying $|S_k| = |S_{k-1}|$.

else

 Set $|S_k| \leftarrow \lceil \rho' |S_k| \rceil$, where $\rho' = \frac{\sum_{\xi \in S_k} \|R(x_k; \xi) - R_{S_k}(x_k)\|^2}{\theta^2 (|S_k| - 1) |S_k| \|R_{S_k}(x_k)\|^2}$.

 Obtain additional i.i.d. samples for S_k and recompute d_{S_k} .

until until a convergence test is satisfied

Remark 4.1. One could also propose other alternatives to [Condition 4](#). For instance, one could follow Bollapragada et al. [\[8\]](#) and derive conditions which lead to a probabilistic threshold on $R_{S_k}(x_k)$ pointing in the same direction as $R(x_k)$. For sake of space, we do not include any algorithms based on this approach. The interested reader is referred to [\[8, 47\]](#) for further details on how such algorithms could be constructed.

5. Risk-averse problems. In this section, we describe how to extend the algorithms above to stochastic programs involving the conditional value-at-risk. We present two different approaches which achieve these ends; both involve a regularization technique proposed in [\[29\]](#) and rewriting $\text{CVaR}_\beta(X)$ as the solution of an auxiliary optimization problem; see [\(5.1\)](#), below. Our first method follows a well-established course of action in risk-averse stochastic programming [\[29, 30, 44\]](#) and conforms to the assumptions used in the previous two sections. Our second method involves solving an additional one-dimensional optimization problem at each iteration.

5.1. Conditional value-at-risk. Let $\Psi_X(x) := \mathbb{P}(X \leq x)$ denote the cumulative distribution function (CDF) of a random variable X . The value-at-risk (VaR) of X , at confidence level $0 < \beta < 1$, also known as the β -quantile, is defined by

$$\text{VaR}_\beta(X) := \inf \{t \in \mathbb{R} : \Psi_X(t) \geq \beta\}.$$

The conditional value-at-risk (CVaR) of X , at confidence level β , is essentially the expected value of X beyond $\text{VaR}_\beta(X)$. Indeed, if $\Psi_X(x)$ is right-continuous, then $\text{CVaR}_\beta(X)$ is precisely the conditional expectation $\mathbb{E}[X|X > \text{VaR}_\beta(X)]$. This implies that $\text{CVaR}_\beta(X) \geq \mathbb{E}[X]$. In order to accommodate more general CDFs, one may alternatively define $\text{CVaR}_\beta(X)$ as the weighted integral of the value-at-risk over the interval $(\beta, 1)$,

$$\text{CVaR}_\beta(X) := \frac{1}{1-\beta} \int_\beta^1 \text{VaR}_\alpha(X) d\alpha.$$

Since $\text{VaR}_\alpha(X)$ is a non-decreasing function of α , note that

$$\text{CVaR}_\beta(X) \geq \frac{1}{1-\beta} \text{VaR}_\beta(X) \int_\beta^1 d\alpha = \text{VaR}_\beta(X).$$

In many applications, $\text{CVaR}_\beta(X)$ is a more useful measure of risk than $\text{VaR}_\beta(X)$ simply because controlling expected failure states is more important than simply controlling the most optimistic failure state. For instance, consider when X can be identified with a stress acting on/within a physical system. In such scenarios, lower values of X are generally preferable to higher values of X . Thus, $\text{VaR}_\beta(X)$ represents the most optimistic value that X can achieve in the worst $(1-\beta) \cdot 100$ percent of possible events. Alternatively, $\text{CVaR}_\beta(X)$ represents the expected value of X in the worst $(1-\beta) \cdot 100$ percent of possible events.

The properties above make $\text{CVaR}_\beta(X)$ a suitable risk measure for industrial optimization problems [41]. There are a variety of ways to treat stochastic programs which incorporate the CVaR [16, 29]. However, in this work, we find that the following “dual formulation” is particularly useful.

In [38] it is shown that $\text{CVaR}_\beta(X)$ can be interpreted as the solution of a scalar optimization problem; namely,

$$(5.1) \quad \text{CVaR}_\beta(X) = \inf_{t \in \mathbb{R}} \left\{ t + \frac{1}{1-\beta} \mathbb{E}[(X-t)_+] \right\},$$

where $(x)_+ := \max\{0, x\}$. Therefore, the stochastic program

$$(5.2) \quad \min_{x \in C} F(x) = \text{CVaR}_\beta[f(x; \xi)]$$

can be conveniently reformulated as

$$(5.3) \quad \min_{(x,t) \in C \times \mathbb{R}} F(x, t) = \mathbb{E} \left[t + \frac{1}{1-\beta} (f(x; \xi) - t)_+ \right].$$

It is well-known that non-smoothness of the operator $(\cdot)_+$, implies non-smoothness of the objective function $F(x, t)$ [38]. Therefore, (5.3) is often solved with subgradient types methods; see, e.g., [43]. An alternative option is to replace CVaR_β by a smooth approximation, which maintains many of its essential properties. In this work, we choose to use a smoothing technique proposed by Kouri and Surowiec [29].

5.2. Smoothing. The non-differentiability of $F(x, t)$ can be circumvented by regularizing the $(\cdot)_+$ function. In [29, Section 4.1.1.], several strategies are proposed. We choose the smooth approximation $(\cdot)_+^\varepsilon$ defined as follows:

$$(y)_+^\varepsilon = y + \varepsilon \ln \left(1 + \exp \left(\frac{-y}{\varepsilon} \right) \right).$$

Likewise, we replace the non-smooth CVaR_β risk measure by the smoothed risk measure

$$(5.4) \quad \text{CVaR}_\beta^\varepsilon(X) = \inf_{t \in \mathbb{R}} \left\{ t + \frac{1}{1-\beta} \mathbb{E}[(X - t)_+^\varepsilon] \right\}$$

and replace (5.3) by

$$(5.5) \quad \min_{(x,t) \in C \times \mathbb{R}} F^\varepsilon(x, t) = \mathbb{E} \left[t + \frac{1}{1-\beta} (f(x; \xi) - t)_+^\varepsilon \right].$$

All of the conclusions in the previous sections carry over to the regularized CVaR problem because the objective function $F^\varepsilon(x, t)$ is now smooth. This means that Algorithm 1 can be used to solve (5.5). It is also important to point out that this smooth CVaR formulation enjoys the advantage that many of the original CVaR properties are preserved, including convexity and monotonicity [29]. Accordingly, if $f(x; \xi)$ is convex for almost every ξ , then $F^\varepsilon(x, t)$ is also convex.

Remark 5.1. The regularization constant ε is a problem-dependent parameter which must be tuned. To guide the tuning process, one may use Lemma 4.3 in [29], which shows that

$$|\text{CVaR}_\beta^\varepsilon(X) - \text{CVaR}_\beta(X)| \leq \frac{\log 2}{1-\beta} \varepsilon.$$

Thus, the value of ε necessary to achieve an intended relative error will depend on both the magnitude of $\text{CVaR}_\beta(X)$ and the confidence level β . A short study on the influence of ε is carried out in [47, Chapter 5.1.3].

Remark 5.2. The function $(\cdot)_+$ falls into a special class of functions so-called “scalar regret functions” [40]; specifically, functions $v : \mathbb{R} \rightarrow \overline{\mathbb{R}}$ which are closed, convex, increasing, and satisfy $v(0) = 0$ and $v(x) > x$ for all $x \neq 0$. If one replaces $\frac{1}{1-\beta}(\cdot)_+^\varepsilon$ in (5.5), with any scalar regret function $v(\cdot)$, then one arrives at an important class of risk-averse stochastic programs, which has also received a great deal of attention [2, 30, 40]:

$$\min_{x \in C} F(x) = \mathcal{R}[f(x; \xi)] \quad \text{where} \quad \mathcal{R}(X) = \inf_{t \in \mathbb{R}} \left\{ t + \mathbb{E}[v(X - t)] \right\}.$$

If v is also smooth, then Algorithm 1 may also be used without further modification to solve this entire family of risk-averse stochastic programs.

5.3. Nested quantile estimation. Although Algorithm 1 can be used to solve (5.5), when there are only a small number of samples, the initial error may be quite large; cf. Subsection 6.2.2. For this reason, we introduce an alternative algorithm. We begin with two observations.

It is well-known that the unique minimizer of (5.1), t^* , is simply the value-at-risk; namely,

$$\text{CVaR}_\beta(X) = t^* + \frac{1}{1-\beta} \mathbb{E}[(X - t^*)_+], \quad \text{where} \quad t^* = \text{VaR}_\beta(X).$$

Accordingly, if we assume that $\text{VaR}_\beta(f(x; \xi))$ was somehow determined *a priori*, it would be possible to rewrite (5.2) as

$$(5.6) \quad \min_{x \in C} \tilde{F}(x) = \mathbb{E}[(f(x; \xi) - \text{VaR}_\beta(f(x; \xi)))_+].$$

This technique of rewriting (5.2) is analogous to the scalar regret function reformulation of stochastic programs involving the entropic risk measure; see, e.g., [30, Section 2.4.2].

It turns out that there are a large number of methods to estimate quantiles which are widely available in scientific software such as R [36], Python (specifically, SciPy [48]), and Julia [4]. Any of these approximations could be substituted for $\text{VaR}_\beta(f(x; \xi))$ in (5.6), once a set of samples of $f(x; \xi)$ is collected. Nevertheless, we choose to approximate the value-at-risk by estimating t^* at each iteration and then solving the regularized form of (5.6). That is, we first compute

$$(5.7) \quad t_{S_k} = \arg \min_{t \in \mathbb{R}} \left\{ t + \frac{1}{1-\beta} \frac{1}{|S_k|} \sum_{\xi_i \in S_k} (f(x; \xi_i) - t)_+^\varepsilon \right\}$$

with a root finding algorithm. This is no more expensive than a standard line search and generally cheaper than applying $P(\cdot)$. Furthermore, one may argue that $t_{S_k} \rightarrow t^*$ as $|S_k| \rightarrow \infty$. We then compute the new iterate $x_{k+1} = Q_{S_k}(x_k)$ via the subsampled gradient map of

$$\tilde{F}_{S_k}^\varepsilon(x) := \frac{1}{|S_k|} \sum_{\xi_i \in S_k} (f(x; \xi_i) - t_{S_k})_+^\varepsilon.$$

The entire adaptive sampling process is described in [Algorithm 3](#), below.

Algorithm 3: Nested quantile estimation and adaptive sampling with CVaR

input : x_0 , step size $\alpha > 0$, initial sample set S_0 , constant $\theta > 0$
 Set $k \leftarrow 0$.
repeat
 Compute $t_{S_k} = \arg \min_{t \in \mathbb{R}} \left\{ t + \frac{1}{1-\beta} \frac{1}{|S_k|} \sum_{\xi_i \in S_k} (f(x_k; \xi_i) - t)_+^\varepsilon \right\}$.
 Update $x_{k+1} = \arg \min_{y \in C} \left\{ \tilde{F}_{S_k}(x_k) + \langle \nabla \tilde{F}_{S_k}(x_k), y - x_k \rangle + \frac{1}{2\alpha} \|y - x_k\|^2 \right\}$.
 if *Test 1 is not satisfied* **then**
 Construct S_{k+1} obeying (3.2).
 else
 Construct S_{k+1} satisfying $|S_{k+1}| = |S_k|$.
 Set $k \leftarrow k + 1$.
until *until a convergence test is satisfied*

6. Numerical examples. In this section, we conduct three different sets of experiments of increasing complexity. We begin with a simple example problem which allows us to test the theory presented in [Subsection 2.4](#). Subsequently, we assess the practicality and robustness of the adaptive sampling algorithms with a risk-averse portfolio optimization application. Finally, we consider the design of a thin steel shell structure with physical model uncertainties.

6.1. Basic example. Our first stochastic programming example is inspired by [43, Section 6.2]. Consider a function

$$(6.1) \quad f(x; \xi) = \sum_{l=1}^{20} a_l (x^l - b_l \xi^l)^2, \quad x = (x^1, \dots, x^{20}), \quad \xi = (\xi^1, \dots, \xi^{20}),$$

where the coefficients $a_l \sim \text{Unif}(1, 2)$ and $b_l \sim \text{Unif}(-1, 1)$ have been randomly sampled once for the sake of simulation and, thereafter, left fixed. Next, assume that ξ is a random vector where each coefficient $\xi^l \sim \text{Unif}(0, 1)$. Finally, define the admissible set $C = [0, \infty)^{20}$, which is closed, convex, and unbounded.

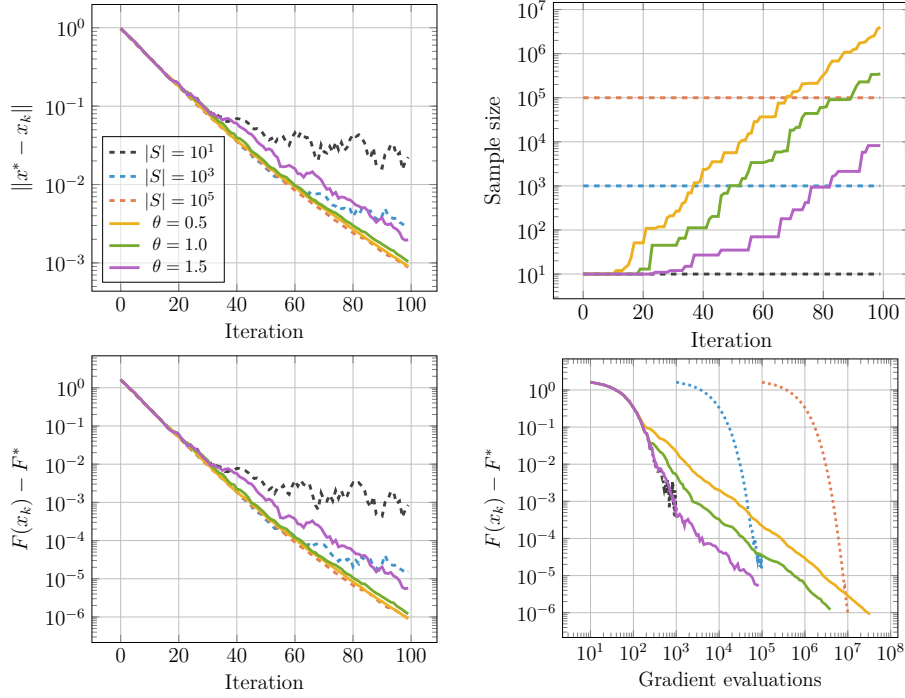


Figure 6.1: Comparison of the stochastic approximation with fixed sample sizes and [Algorithm 1](#) applied to the stochastic program (6.2). The top-left and bottom-lefts plot shows the error in the solution vs. the iteration number and the error in the objective function vs. the iteration number, respectively. Here, it is clear that the fixed sample size examples, $|S| = 10^1$, 10^3 , eventually stop converging. Eventually, this would also happen to the $|S| = 10^5$ example. The top-right plot demonstrates an exponential growth in the samples sizes with [Algorithm 1](#). The bottom-right plot shows the error in the objective function vs. the cumulative number of gradient evaluations.

With the definitions given above, we consider the (risk-neutral) stochastic program

$$(6.2) \quad \min_{x \in C} \left\{ F(x) = \mathbb{E}[f(x; \xi)] \right\}.$$

Note that this program is strongly convex and that $f(x; \xi)$ is differentiable for every $\xi \in \Xi = [0, 1]^{20}$. Therefore, there exists a unique global minimizer and [Theorem 2.8](#) applies. In fact, the unique global minimizer $x^* = (x^{*,1}, \dots, x^{*,20})$ of (6.2) can be written out explicitly; i.e., $x^{*,l} = \max\{0, b_l/2\}$, for each $l = 1, \dots, 20$.

This example has two purposes: first, to verify the theory presented in [Subsection 2.4](#) and, second, to compare the performance of [Algorithm 1](#) with different values of θ . In [Figure 6.1](#) we see the results from six representative optimization runs. The first three runs use fixed sample sizes of $|S_k| = 10$, 10^3 , and 10^5 , respectively, for all iterations k ; these runs imitate naive approaches to compare against. The subsequent three runs each begin with the common initial batch size $|S_0| = 10$ and are executed using [Algorithm 1](#) with the parameter values $\theta = 0.5$, 1.0 , and 1.5 , respectively. All of the runs use a fixed step size of $\alpha = 0.025$. Due to [Theorem 2.8](#), similar results are expected for all step sizes $\alpha < 1/L$ and sufficiently small $\theta > 0$.

The leftmost plots in [Figure 6.1](#) illustrate q-linear convergence for each of the adaptive sampling runs, albeit, at different levels of efficiency. Recalling [Theorem 2.8](#), this is the best

outcome one could hope for. For all smaller values of $\theta > 0$, the algorithm continues to converge linearly, however, for larger values of θ , the convergence eventually breaks down. The value of θ where linear convergence fails depends on the step size α , as one would expect from [Theorem 2.8](#). These plots also show that stochastic approximation methods with a fixed step size and sample size eventually stop converging.

As a rule of thumb in choosing θ , we suggest that one starts with a value around 1.0 and then tracks the adaptive algorithm until the first significant growth in the sample size plateaus. If there has already been a meaningful decrease in the objective value by this point, keep θ fixed; otherwise, θ should probably be decreased moderately. In all cases we have looked at, a reasonable value for θ can be chosen based on the behavior of the algorithm in its first 10 to 20 iterations.

6.2. Portfolio optimization. With this set of optimization problems, we continue to illustrate the practicality of the adaptive sampling algorithm proposed above. Specifically, we choose to focus on a class of archetypal operations research problems taken from [\[43, Section 6.1\]](#). This example is the first of ours to incorporate the paradigm of risk-averse stochastic optimization; cf. [Section 5](#).

6.2.1. Problem description. Let us consider a random cost model with $n = 100$ financial instruments whose outputs are each given as $\xi = A + Bu$. In this model, A is a n -dimensional vector representing the expected rate of return of a single instrument and B is an $n \times n$ -dimensional matrix which correlates the uncertainty in this return. Each component of A is defined through an independent sample of a uniform distribution over $[0.9, 1.2]$ and, likewise, each entry in B is defined by an independent sample of a uniform distribution over $[0, 0.1]$. As with the model parameters a_l and b_l appearing in [\(6.1\)](#), both A and B only specify parameters in the model. Therefore, A and B are randomly generated and then held fixed throughout the entire optimization process. Finally, each component of the n -dimensional random vector u , which itself acts to introduce uncertainty in the model, is taken to be independent and obey a standard normal distribution.

Given the financial instrument model described above, we now consider the investment of one share of wealth distributed over the $n = 100$ independent random financial instruments. We choose to denote the amount of investment into the l -th asset by $x^l \geq 0$, whereby $\sum_{l=1}^{100} x^l = 1$. Accordingly, we arrive at the following (stochastic) loss function:

$$(6.3) \quad f(x; \xi) = - \sum_{l=1}^{100} \xi^l x^l,$$

where $x = (x^1, \dots, x^{100})$ is our given portfolio allocation strategy.

Let us say that we would like to minimize the loss over all portfolio strategies which have an expected return no smaller than 1.05. We therefore define the following admissible set of normalized portfolios:

$$C = \left\{ x \in \mathbb{R}^{100} : x^l \geq 0, \quad \sum_{l=1}^{100} x^l = 1, \quad \sum_{l=1}^{100} A_l x^l \geq 1.05 \quad l = 1, \dots, 100 \right\}.$$

In a risk-neutral paradigm, we seek only to minimize the expected value of [\(6.3\)](#) over C . The corresponding stochastic program is simply

$$(6.4) \quad \min_{x \in C} \left\{ F(x) = \mathbb{E}[f(x; \xi)] \right\}.$$

With this definition of $F(x)$, the strong convexity assumption made in [Theorem 2.8](#) is not satisfied.

It turns out that the expected loss problem above tends not to serve well for most practical investment decisions. Alternatively, one can minimize the loss with CVaR_β as a risk measure; this is a common choice in financial applications [19, 21]. Accordingly, we focus on the following class of risk-averse stochastic programs:

$$(6.5) \quad \min_{x \in C} \left\{ F_\beta(x) = \text{CVaR}_\beta[f(x; \xi)] \right\},$$

where $\beta \in [0, 1)$ is the risk-averseness parameter. Note that $F(x) = F_0(x)$ in the notation of (6.4) and (6.5), and so the risk-neutral program (6.4) has not actually been ignored [38, 39].

Remark 6.1. As already pointed out in Section 5, the CVaR risk measure introduces non-smoothness into the objective functional which commonly breaks the convergence of traditional gradient descent algorithms. Therefore we follow Subsection 5.2 in our experiments and replace the CVaR in (6.5) by the risk measure $\text{CVaR}_\beta^\varepsilon$, defined in (5.4), with some small regularization parameter $\varepsilon > 0$.

6.2.2. Risk-averse portfolio optimization. In our first set of portfolio optimization experiments, we compare the performance of Algorithm 1 on the stochastic program (6.5), for a variety of risk-averseness parameters $\beta > 0$. Recall (5.4) and note that each of these problems may be written as

$$(6.6) \quad \min_{(x, t) \in C \times \mathbb{R}} \left\{ F_\beta(x, t) = t + \frac{1}{1 - \beta} \mathbb{E}[(f(x; \xi) - t)_+]^\varepsilon \right\},$$

after regularization. Because our experiments in Subsection 6.1 already indicated a robustness with respect to the algorithm parameter θ , we choose to focus our attention here on its sensitivity to the risk-averseness parameter β . In this example, we consider $\beta = 0, 0.5, 0.9$, and 0.95 . For all $\beta > 0$, we set $\varepsilon = 0.1$.

Note that β actually changes the optimization problem. Hence, for each β , we choose a different sampling rate parameter θ . For $\beta = 0$ and $\beta = 0.5$, we set $\theta = 2.0$; for $\beta = 0.9$, we take $\theta = 1.5$; and for $\beta = 0.95$, we specify $\theta = 0.125$. These parameters were chosen to promote comparable growth of the sample size across the different cases. Generally, as $\beta < 1$ grows, θ should shrink.

Figure 6.2 presents the results of our numerical experiments. When the risk averseness parameter β is increased, we expect that the achieved objective value increases too. This feature is clearly observed in Figure 6.2. It is also evident from Figure 6.2 that the initial value of the objective function, $F_\beta(x_0, t_0)$, gets progressively farther from its optimal value as β grows. This is largely due to the fact that the same initial value of the auxiliary variable, $t = t_0$, has been used in each experiment. In light of Subsection 5.3, one could instead just setting t_0 to be the solution of (5.7). This is essentially what is done in Algorithm 3, except it goes further by resetting the value of t as the solution of (5.7) at each iteration.

6.2.3. Risk-averse portfolio optimization with Algorithm 3. Here, we briefly compare Algorithm 3 to Algorithm 1. Since the setting $\beta = 0$ simply amounts to problem (6.4), our comparison only involves $\beta = 0.5, 0.9$, and 0.95 . It may be seem natural to also choose the same values of θ used in Subsection 6.2.2, however, we found that the auxiliary variable t appearing in (6.6) has a strong effect on variance of the objective function. Because the gradient with respect to t does not appear in Algorithm 3, we were able to use larger values of θ than in Subsection 6.2.2 and this tended to result in better sample size efficiency. To be specific, for $\beta = 0.5$, we set $\theta = 3.0$; for $\beta = 0.9$, we set $\theta = 4.0$; and for $\beta = 0.95$, we set $\theta = 4.5$.

The results of our comparison are presented in Figure 6.3. Evidently, both algorithms converge to the same optimal objective value. Although Algorithm 3 involves solving a one-

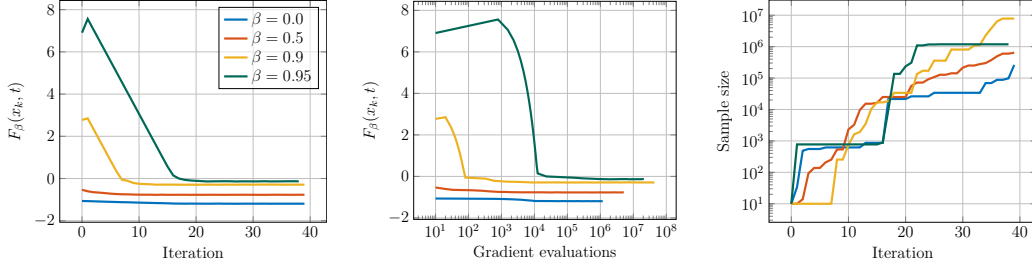


Figure 6.2: Numerical results for the portfolio optimization problem (6.5) for the risk-averseness parameters $\beta = 0.0$ (which also corresponds to the risk-neutral problem (6.4)), 0.5, 0.9, and 0.95. On the left, we see the value of the objective function converge with respect to the iteration number. In the middle, we see the value of the objective function converge with respect to the cumulative number of gradient evaluations. On the right, we see the sample size grow with respect to the iteration number.

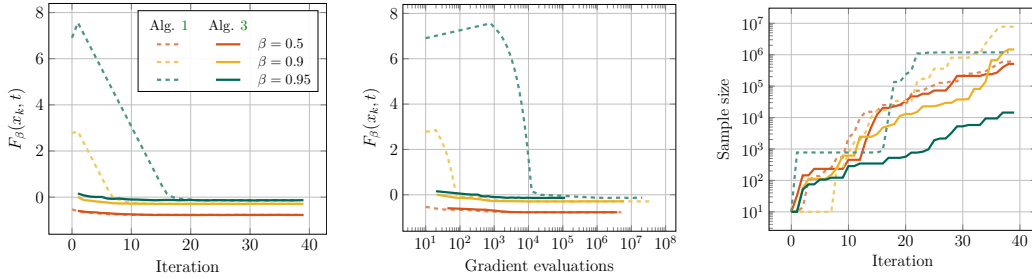


Figure 6.3: Numerical results for problem (6.5), with $\beta = 0.5$, 0.9, and 0.95, comparing Algorithms 1 and 3.

dimensional optimization problem at each iteration, it also appears to generate fewer samples which could make it more efficient overall in some applications.

6.3. Shape optimization of shell structures. We now turn our attention towards a problem in engineering shape design. It is well-accepted that shape optimization problems are difficult to characterize as well as solve and often involve significant engineering oversight [7]. The intention in such problems is usually not to seek a globally optimal design, but instead to begin with an initial “good” design and find a nearby local optimum, which improves on a specified quantity of interest. Because of its potential to be more efficient, an SQP approach based on Algorithm 3 is used in this final example.

Our chosen example centers on the question of how to find the shape of a steel shell which minimizes some measurement of the internal strains resulting from a specified distribution of external loads. For the initial shape, we choose a half-cylinder on its side, as depicted in Figure 6.4. We assume that an uncertain load \mathbf{f} will be applied to the shell structure from above and that the final manufactured thickness t of the shell is also uncertain. To simplify our implementation, we assume that every cross-section of the applied load follows a simple bell shape profile along the major axis of the shell and that the uncertainty in the load lies only in the position where it achieves its maximum. More specifically, we model the applied load (measured in Newtons) by the vector field

$$\mathbf{f}(x, y, z) = -10^5 \exp\left(-(x - 6 + 4a/3)^2\right) \mathbf{e}_z, \quad \text{with } a \sim \mathcal{N}(0, 1), \quad \mathbf{e}_z = (0, 0, 1),$$

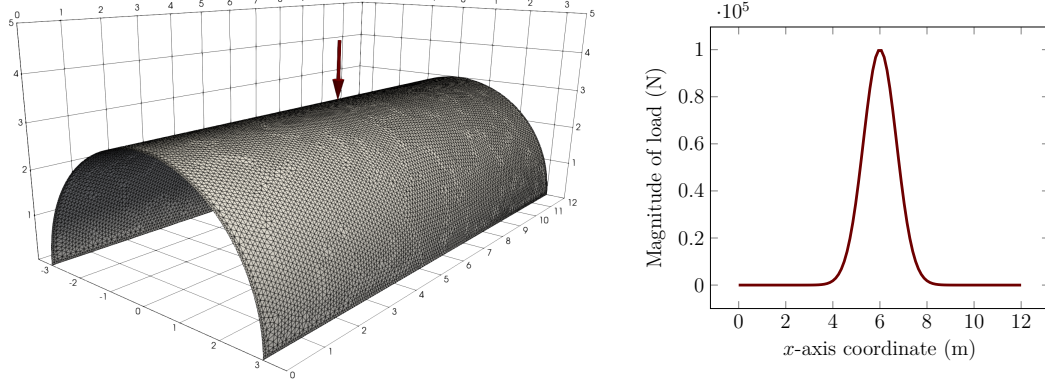


Figure 6.4: Initial design of shell structure and applied force, \mathbf{f} , when $a = 0$.

and all distances measured in units of meters (m); cf. [Figure 6.4](#). Furthermore, we model the uncertain shell thickness by the uniformly distributed random variable

$$t \sim \text{Unif}(4.05 \text{ cm}, 5.05 \text{ cm}).$$

It is of course possible to consider other uncertain model parameters, in addition to the thickness. In this example, however, we choose to fix the mass density ($7.85 \cdot 10^3 \text{ kg m}^{-3}$), Young's modulus ($2.069 \cdot 10^{11} \text{ Pa}$), and Poisson's ratio ($2.9 \cdot 10^{-1}$) of the steel shell structure, judging them to be far less sensitive sources of uncertainty.

Our goal here is to find a geometry parameterization x which optimizes the shell's internal energy $\Pi(x) = \Pi(x; \mathbf{f}, t)$, subject to the stochastic load \mathbf{f} and thickness t , given above. In order to arrive at a realistic and practical optimum, we only look at a set of similarly expensive geometries — namely, those having (i) equal surface area — and physically reasonable geometries, wherein (ii) the supporting sides of the shell structure remain on the ground and (iii) the open open ends of the structure stay perpendicular to the ground. These three sets of constraints lead to an abstract design space C and an associated stochastic optimization problem, which may be compactly written as

$$(6.7) \quad \min_{x \in C} \left\{ F(x) = \mathcal{R}[\Pi(x)] \right\},$$

where \mathcal{R} is a given risk measure. We only consider $\mathcal{R} = \text{CVaR}_{\beta}^{\varepsilon}$, where $\beta \in [0, 1)$ and $\varepsilon \geq 0$.

It is common practice to represent the design geometry by the position of the nodes in its finite element representation [\[6\]](#). These nodes, in turn, serve as control variables $x \in \mathbb{R}^n$, which may be updated along their physical normals at each step in the optimization algorithm [\[7\]](#). In this example, we follow the semi-analytical adjoint-based procedure outlined in [\[7, Subsection 5.5.4\]](#) and implemented in the KratosMultiphysics Structural Mechanics and Shape Optimization Application [\[17\]](#). The geometry update rule we employ at the end of each optimization step k uses sophisticated filtering techniques and mesh movement algorithms outlined in [\[6\]](#).

Following [\[7\]](#), for each independent pair of load and thickness realizations, \mathbf{f}_i and t_i , the calculation of the corresponding strain energy realization, $\Pi_i(x_k) = \Pi(x_k; \mathbf{f}_i, t_i)$, together with its gradient, $\nabla \Pi_i(x_k)$, involves the discrete solution of two partial differential equations (PDEs). In this study, we choose to represent the shell using the classical three-parameter Kirchhoff-Love PDE model and form a discretization of it with lowest-order C^0 -continuous finite elements;

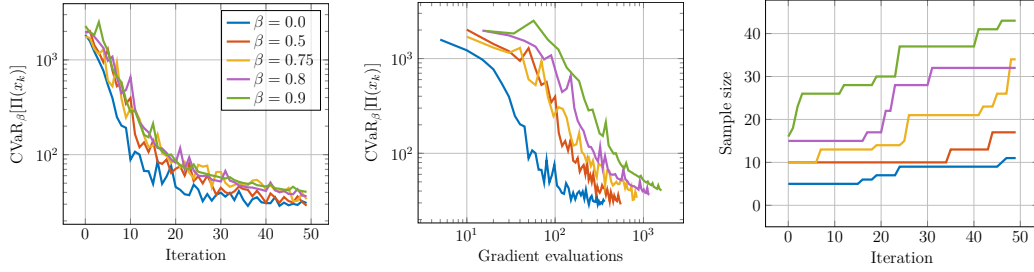


Figure 6.5: Optimization logs for the design optimization problem of shell structures (6.7) with $\beta = 0, 0.5, 0.75, 0.8$, and 0.9 . In all cases, the algorithm parameters $\alpha = 0.1$ and $\theta = 0.8$ were used. On the left, we see the convergence in the value of the objective function vs. the iteration number. In the middle, we see the convergence in the value of the objective function vs. the cumulative number of gradient evaluations. On the right, we see the growth in the sample size vs. iteration number.

cf. [5]. In particular, we use three-node ANDES elements [20] on the ($n = 13783$)-node simplicial mesh depicted in Figure 6.4.

We performed five numerical shape design optimization experiments with the discretization just described. The first experiment used $\beta = \varepsilon = 0$. The second, third, fourth, and fifth used $\beta = 0.5, 0.75, 0.8$, and 0.9 respectively, each with $\varepsilon = 0.1$. In the risk-neutral case (i.e., $\beta = 0$, $\mathcal{R} = \mathbb{E}$), we began with an initial batch size of $|S_0| = 5$. In each of the risk-averse cases (i.e., $\beta > 0$, $\mathcal{R} = \text{CVaR}_\beta^\varepsilon$), we began with $|S_0| = 10$. In every experiment, we used the step size $\alpha = 0.1$ and the sampling rate parameter $\theta = 0.8$.

Each of the optimization problems were solved using the SQP approach introduced in Section 4. For the risk-neutral problem, $\beta = 0$, we used Algorithm 2. However, for the CVaR problems, $\beta > 0$, we modified the algorithm with the nested quantile estimation strategy described in Subsection 5.3. For further details, see [47, Chapter 4.5]. In each experiment, the stochastic optimization algorithm was stopped after 50 iterations. Plots of the optimization logs are given in Figure 6.5 and the final geometries are shown in Figure 6.6. For visual comparison, we also present the final geometry one would find by optimizing the shell if it had exactly the expected thickness $t = 5.00$ cm and exactly the expected stress, $\mathbf{f}(x, y, z) = -10^5 \exp(-(x - 6)^2) \mathbf{e}_z$, was being applied (i.e., $a = 0.0$ m). The interested reader may also refer the reader to [47] for additional shape optimization experiments.

In Figure 6.5, we see that the objective value in each stochastic setting decreases significantly throughout the course of optimization. As usual, the more risk-averse the problem, the more samples are required. In fact, in the risk-neutral setting, $\beta = 0$, just 10 samples is easily enough to fulfill Test 2 throughout nearly the entire course of the optimization. This is the reason we present results for this experiment which begin with fewer than 10 samples. Using fewer than 10 samples for the risk-averse experiments did not lead to predictable growth in the initial sample sizes. This is likely because of a large error in estimating the corresponding quantiles using (5.7) with very few samples.

Evidently, the various optimization problems deliver distinctly different optimal shapes. The risk-neutral design in Figure 6.6 (b) is better-suited to the more likely but less damaging loads centered on the middle of the structure. This is most evident when it is compared to the optimal design in Figure 6.6 (a), which comes from the deterministic scenario where the load is centered on middle of the structure with absolute certainty. On the other hand, the risk-averse designs Figures 6.6 (c)–6.6 (f) are progressively better suited to the less likely, but more damaging, loads centered near the ends of the structure. Initially, as β grows, we witness

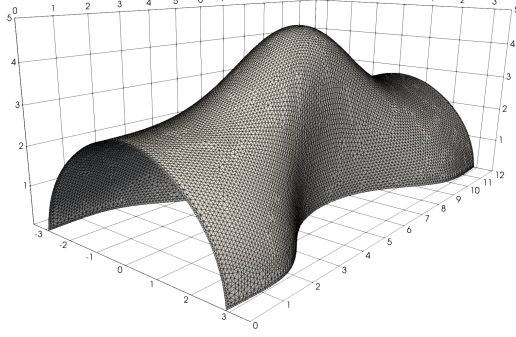
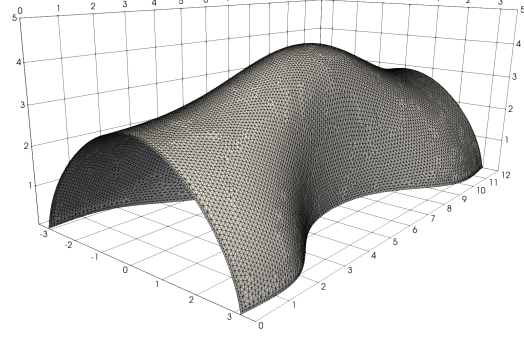
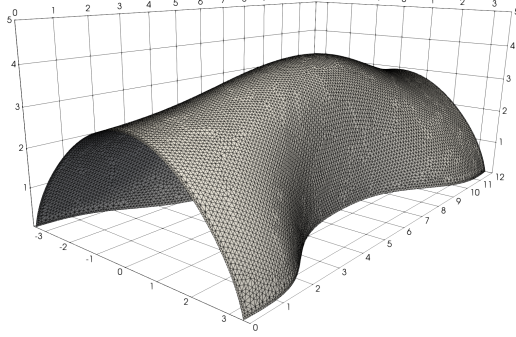
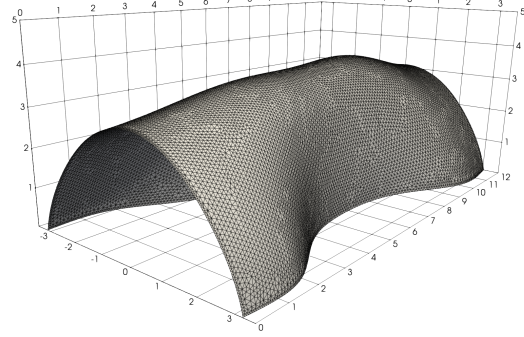
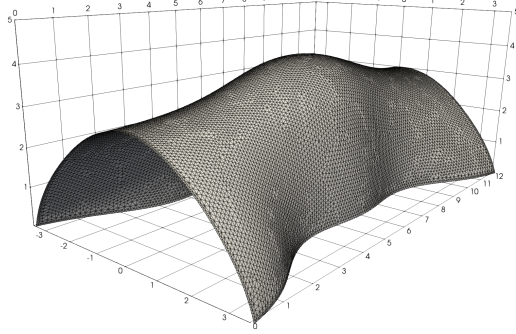
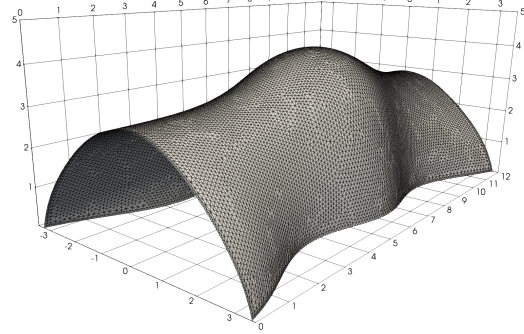
(a) Final shell design when $a = 0.0$ m, $t = 5.00$ cm.(b) Final shell design when $\mathcal{R} = \mathbb{E}$ (c) Final shell design when $\mathcal{R} = \text{CVaR}_{0.5}$ (d) Final shell design when $\mathcal{R} = \text{CVaR}_{0.75}$ (e) Final shell design when $\mathcal{R} = \text{CVaR}_{0.8}$ (f) Final shell design when $\mathcal{R} = \text{CVaR}_{0.9}$

Figure 6.6: Final shell designs for deterministic, risk-neutral, and risk-averse optimization problems.

progressively flatter bumps in the center of the structure until a new type of shape appears somewhere around $\beta = 0.75$. This indicates a change in the local minima landscape. Likely there are two nearby local minima in this region, one that is a continuation of the risk-neutral minimum and a second local minimum influenced by the extreme values of the stress $\Pi(x)$. Additional numerical experiments (not included here) indicate to us that the basin of attraction of the new state exhibited in Figures 6.6 (e) and 6.6 (f) grows with $\beta > 0.75$. At the same time,

the basin of attraction of the original risk-neutral category of designs appears to shrink and eventually vanish.

7. Conclusion. This paper deals with stochastic optimization algorithms with dynamic samples sizes. We focus on a large class of stochastic programs with deterministic constraints. In doing so, we pose sufficient conditions on the sample sizes which guarantee that a class of adaptive sampling methods converge. We then introduce practical tests to check these conditions and illustrate their robustness in contemporary applications, including engineering design with physical model uncertainties. Our methods not only apply to risk-neutral optimization problems; that is, when the objective function is the expected value of some stochastic quantity. Indeed, using the conditional value-at-risk (CVaR) as a working example, we show how a large family of risk-averse problems can be treated with the strategies developed here.

Acknowledgments. The authors acknowledge the computer resources on MareNostrum and Salomon provided by the Barcelona Supercomputing Center (IM-2019-2-0008) and the Czech Republic Ministry of Education, Youth and Sports (from the Large Infrastructures for Research, Experimental Development, and Innovations project “e-INFRA CZ – LM2018140”), respectively. This work was performed under the auspices of the U.S. Department of Energy by Lawrence Livermore National Laboratory under Contract DE-AC52-07NA27344, LLNL-JRNL-827097.

REFERENCES

- [1] P. ARTZNER, F. DELBAEN, J.-M. EBER, AND D. HEATH, *Coherent measures of risk*, Mathematical finance, 9 (1999), pp. 203–228.
- [2] A. BEN-TAL AND M. TEOULLE, *Expected utility, penalty functions, and duality in stochastic nonlinear programming*, Management Science, 32 (1986), pp. 1445–1466.
- [3] D. P. BERTSEKAS AND A. SCIENTIFIC, *Convex optimization algorithms*, Athena Scientific Belmont, 2015.
- [4] J. BEZANSON, A. EDELMAN, S. KARPINSKI, AND V. B. SHAH, *Julia: A fresh approach to numerical computing*, SIAM review, 59 (2017), pp. 65–98, <https://doi.org/10.1137/141000671>.
- [5] M. BISCHOFF, E. RAMM, AND J. IRSLINGER, *Models and finite elements for thin-walled structures*, Encyclopedia of Computational Mechanics Second Edition, (2018), pp. 1–86.
- [6] K.-U. BLETZINGER, *A consistent frame for sensitivity filtering and the vertexassigned morphing of optimal shape*, Struct Multidisc Optim, 49 (2014), pp. 873–895.
- [7] K.-U. BLETZINGER, *Shape Optimization*, 2017, <https://doi.org/10.1002/9781119176817.ecm2109>.
- [8] R. BOLLAPRAGADA, R. H. BYRD, AND J. NOCEDAL, *Adaptive Sampling Strategies for Stochastic Optimization*, SIAM J. Optim., 28 (2018), pp. 3312–3343.
- [9] R. BOLLAPRAGADA, R. H. BYRD, AND J. NOCEDAL, *Exact and inexact subsampled Newton methods for optimization*, IMA J. Numer. Anal., 39 (2019), pp. 545–548, <https://doi.org/10.1093/imanum/dry009>, <https://arxiv.org/abs/1609.08502>.
- [10] R. BOLLAPRAGADA, D. MUDIGERE, J. NOCEDAL, H. J. M. SHI, AND P. T. P. TANG, *A Progressive Batching L-BFGS Method for Machine Learning*, 35th Int. Conf. Mach. Learn. ICML 2018, 2 (2018), pp. 989–1013, <https://arxiv.org/abs/1802.05374>.
- [11] L. BOTTOU, F. E. CURTIS, AND J. NOCEDAL, *Optimization methods for large-scale machine learning*, Siam Review, 60 (2018), pp. 223–311.
- [12] R. H. BYRD, G. M. CHIN, J. NOCEDAL, AND Y. WU, *Sample size selection in optimization methods for machine learning*, Mathematical programming, 134 (2012), pp. 127–155.
- [13] C. CARTIS AND K. SCHEINBERG, *Global convergence rate analysis of unconstrained optimization methods based on probabilistic models*, Mathematical Programming, 169 (2018), pp. 337–375.
- [14] A. CHAUDHURI, M. NORTON, AND B. KRAMER, *Risk-based design optimization via probability of failure, conditional value-at-risk, and buffered probability of failure*, in AIAA Scitech 2020 Forum, 2020, p. 2130.
- [15] A. CHAUDHURI, B. PEHERSTORFER, AND K. WILLCOX, *Multifidelity cross-entropy estimation of conditional value-at-risk for risk-averse design optimization*, in AIAA Scitech 2020 Forum, 2020, p. 2129.
- [16] S. CURI, K. Y. LEVY, S. JEGELKA, AND A. KRAUSE, *Adaptive Sampling for Stochastic Risk-Averse Learning*, (2019), <http://arxiv.org/abs/1910.12511>, <https://arxiv.org/abs/1910.12511>.
- [17] P. DADVAND, R. ROSSI, AND E. ONATE, *An Object-oriented Environment for Developing Finite Element Codes for Multi-disciplinary Applications*, Arch. Comput. Methods Eng., 17 (2010), pp. 253–

- 297.
- [18] S. DE, A. YADAV, D. JACOBS, AND T. GOLDSTEIN, *Automated inference with adaptive batches*, in Artificial Intelligence and Statistics, 2017, pp. 1504–1513.
 - [19] K. DOWD, *Measuring market risk*, John Wiley & Sons, 2007.
 - [20] C. A. FELIPPA, *A study of optimal membrane triangles with drilling freedoms*, Computer Methods in Applied Mechanics and Engineering, 192 (2003), pp. 2125–2168.
 - [21] H. FÖLLMER AND A. SCHIED, *Stochastic finance: an introduction in discrete time*, Walter de Gruyter, 2011.
 - [22] M. P. FRIEDLANDER AND M. SCHMIDT, *Hybrid deterministic-stochastic methods for data fitting*, SIAM Journal on Scientific Computing, 34 (2012), pp. A1380–A1405.
 - [23] C. GEIERSBACH, E. LOAYZA-ROMERO, AND K. WELKER, *Stochastic approximation for optimization in shape spaces*, (2020), pp. 1–24, <http://arxiv.org/abs/2001.10786>, <https://arxiv.org/abs/2001.10786>.
 - [24] M. HINZE, R. PINNAU, M. ULBRICH, AND S. ULBRICH, *Optimization with PDE constraints*, vol. 23, Springer Science & Business Media, 2008.
 - [25] T. HOMEM-DE-MELLO, *Variable-sample methods for stochastic optimization*, ACM Transactions on Modeling and Computer Simulation (TOMACS), 13 (2003), pp. 108–133.
 - [26] I. G. ION, Z. BONTINCK, D. LOUKREZIS, U. RÖMER, S. ULBRICH, S. SCHÖPS, AND H. D. GERSEM, *Robust shape optimization of electric devices based on deterministic optimization methods and finite-element analysis with affine parametrization and design elements*, Electr. Eng., 100 (2018), pp. 2635–2647, <https://doi.org/10.1007/s00202-018-0716-6>, <https://doi.org/10.1007/s00202-018-0716-6>.
 - [27] D. P. KOURI, M. HEINKENSCHLOSS, D. RIDZAL, AND B. G. VAN BLOEMEN WAANDERS, *A trust-region algorithm with adaptive stochastic collocation for PDE optimization under uncertainty*, SIAM Journal on Scientific Computing, 35 (2013), pp. A1847–A1879.
 - [28] D. P. KOURI AND A. SHAPIRO, *Optimization of PDEs with Uncertain Inputs*, oct 2018, pp. 41–81, https://doi.org/10.1007/978-1-4939-8636-1_2.
 - [29] D. P. KOURI AND T. M. SUROWIEC, *Risk-averse PDE-constrained optimization using the conditional value-at-risk*, SIAM J. Optim., 26 (2016), pp. 365–396, <https://doi.org/10.1137/140954556>, <http://epubs.siam.org/recursos.biblioteca.upc.edu/doi/pdf/10.1137/140954556>.
 - [30] D. P. KOURI AND T. M. SUROWIEC, *Existence and optimality conditions for risk-averse PDE-constrained optimization*, SIAM-ASA J. Uncertain. Quantif., 6 (2018), pp. 787–815, <https://doi.org/10.1137/16M1086613>.
 - [31] P. KROKHMAL, J. PALMQUIST, AND S. URYASEV, *Portfolio optimization with conditional value-at-risk objective and constraints*, Journal of risk, 4 (2002), pp. 43–68.
 - [32] Y. NESTEROV, *Springer Optimization and Its Applications 137 Lectures on Convex Optimization Second Edition*, 2018, <http://www.springer.com/series/7393>.
 - [33] J. NOCEDAL AND S. WRIGHT, *Numerical optimization*, Springer Science & Business Media, 2006.
 - [34] C. PAQUETTE AND K. SCHEINBERG, *A stochastic line search method with expected complexity analysis*, SIAM Journal on Optimization, 30 (2020), pp. 349–376.
 - [35] R. PASUPATHY, P. GLYNN, S. GHOSH, AND F. S. HASHEMI, *On sampling rates in simulation-based recursions*, SIAM Journal on Optimization, 28 (2018), pp. 45–73.
 - [36] R. CORE TEAM, *R: A Language and Environment for Statistical Computing*, R Foundation for Statistical Computing, Vienna, Austria, 2017, <https://www.R-project.org/>.
 - [37] R. T. ROCKAFELLAR AND J. O. ROYSET, *On buffered failure probability in design and optimization of structures*, Reliab. Eng. Syst. Saf., 95 (2010), pp. 499–510, <https://doi.org/10.1016/j.ress.2010.01.001>.
 - [38] R. T. ROCKAFELLAR AND S. URYASEV, *Optimization of conditional value-at-risk*, J. Risk, 2 (2000), pp. 21–41, <https://doi.org/10.21314/jor.2000.038>.
 - [39] R. T. ROCKAFELLAR AND S. URYASEV, *Conditional value-at-risk for general loss distributions*, Journal of banking & finance, 26 (2002), pp. 1443–1471.
 - [40] R. T. ROCKAFELLAR AND S. URYASEV, *The fundamental risk quadrangle in risk management, optimization and statistical estimation*, Surveys in Operations Research and Management Science, 18 (2013), pp. 33–53.
 - [41] R. T. ROCKAFELLAR AND J. O. ROYSET, *Engineering Decisions under Risk Averseness*, ASCE-ASME J. Risk Uncertain. Eng. Syst. Part A Civ. Eng., 1 (2015), pp. 1–12, <https://doi.org/10.1061/AJRUA6.0000816>.
 - [42] F. ROOSTA-KHORASANI AND M. W. MAHONEY, *Sub-sampled Newton methods*, Mathematical Programming, 174 (2019), pp. 293–326.
 - [43] J. O. ROYSET AND R. SZECHTMAN, *Optimal budget allocation for sample average approximation*, Oper. Res., 61 (2013), pp. 762–776, <https://doi.org/10.1287/opre.2013.1163>.
 - [44] A. SHAPIRO, D. DENTCHEVA, AND A. RUSZCZYŃSKI, *Lectures on Stochastic Programming*, 2009, <https://doi.org/10.1137/1.9780898718751>.
 - [45] R. SHI, L. LIU, T. LONG, AND Y. TANG, *Filter-based adaptive Kriging method for black-box optimization problems with expensive objective and constraints*, Comput. methods applied Mech. Eng.,

- (2018).
- [46] M. ULBRICH AND S. ULBRICH, *Nichtlineare Optimierung*, Springer-Verlag, 2012.
 - [47] S. URBAINCZYK, *Adaptive sampling for stochastic optimization with applications in risk-averse engineering design and machine learning*, master's thesis, Technische Universität München, Germany, 2020.
 - [48] P. VIRTANEN, R. GOMMERS, T. E. OLIPHANT, M. HABERLAND, T. REDDY, D. COUNAPEAU, E. BUROVSKI, P. PETERSON, W. WECKESSER, J. BRIGHT, ET AL., *SciPy 1.0: Fundamental algorithms for scientific computing in Python*, Nature Methods, (2020).
 - [49] Y. XIE, *Methods for Nonlinear and Noisy Optimization*, PhD thesis, Northwestern University, 2021.
 - [50] Y. XIE, R. BOLLAPRAGADA, R. BYRD, AND J. NOCEDAL, *Constrained and composite optimization via adaptive sampling methods*, arXiv preprint arXiv:2012.15411, (2020).
 - [51] H. YANG AND M. GUNZBURGER, *Algorithms and analyses for stochastic optimization for turbofan noise reduction using parallel reduced-order modeling*, Computer Methods in Applied Mechanics and Engineering, 319 (2017), pp. 217–239.
 - [52] Z. ZOU, D. KOURI, AND W. AQUINO, *An adaptive local reduced basis method for solving PDEs with uncertain inputs and evaluating risk*, Computer Methods in Applied Mechanics and Engineering, 345 (2019), pp. 302–322.